

Supporting Information

Contents

Table S1: List of conductivity of some of the reported conductive MOFs in assynthesized, guest-free and iodine-loaded forms

Figure S1: PXRD of **Mn-F**, **Co-F**, **Ni-F** and **Zn-F** MOF

Figure S2: M-O and C-O bond lengths of **Mn-F**, **Co-F** and **Zn-F**

Figure S3: FTIR spectra of **Mn-F**, **Co-F**, **Ni-F** and **Zn-F** MOFs

Figure S4: Calculated band gap (eV) of the MOFs.

Table S2: CO stretching frequency values after and before heating

Figure S5: FTIR spectra showing CO stretching frequency after and before heating for MOFs

Figure S6: Temperature dependent conductivity curves

Figure S7: TGA graph of **Mn-F** MOF

Figure S8: PXRD of (a) **Mn-F** and (b) **Co-F** MOF before and after heating

Figure S9: PXRD of **Ni-F** MOF before and after heating

Figure S10: SEM image of the **Co-F** pellet

Figure S11: Single crystal sizes of the MOFs

Figure S12: Optimized geometries of the Zn, Ni, Mn and Co containing Metal-Organic Frameworks.

Table S3: Crystallographic table

Table S1: List of conductivity of some of the reported conductive MOFs in assynthesized, guest-free and iodine-loaded forms.

MOFs	Assynthesized/ solvated Conductivity (Scm ⁻¹)	Guest-free/ desolvated Conductivity (Scm ⁻¹)	I ₂ loaded conductivity (Scm ⁻¹)	Measurments	E _a (eV)	References
Co ₂ (DOBDC)(DMF) ₂	-	1.5 × 10 ⁻¹³	-	2-probe	0.58	1
Ni ₂ (DOBDC)(DMF) ₂	-	2.8 × 10 ⁻¹⁴	-	2-probe	0.62	
Zn ₂ (DOBDC)(DMF) ₂	-	3.3 × 10 ⁻¹⁴	-	2-probe	0.54	
Mn ₂ (DOBDC)(DMF) ₂	3.9 × 10 ⁻¹³	3.0 × 10 ⁻¹³	-	2-probe	0.55	
Mn ₂ (DSBDC)(DMF) ₂	2.5 × 10 ⁻¹²	1.2 × 10 ⁻¹²	-	2-probe	0.81	3
Cu [Ni(pdt) ₂]	-	1 × 10 ⁻⁸	1 × 10 ⁻⁴	2-probe	-	4
[Co(ebic) ₂] _n	-	2.46 × 10 ⁻⁹	2.21 × 10 ⁻⁷	-	-	5
[Zn(ebic) ₂] _n	-	4.33 × 10 ⁻⁹	3.47 × 10 ⁻⁷	-	-	
[Co _{1.5} (bdc) _{1.5} (H ₂ bpz)]	-	2.59 × 10 ⁻⁹	1.56 × 10 ⁻⁶	2-probe	-	6
[Tb ₃ (Cu ₄ I ₄) ₃ (ina) ₉] _n	-	5.72 × 10 ⁻¹¹	2.16 × 10 ⁻⁴	-	-	7
Cu ₃ HIB ₂	13	-	-	4-probe	-	8
Ni ₃ HIB ₂	8	-	-	4-probe	-	
Ni ₃ HTB ₂	0.15	-	-	2-probe	-	9
Ni ₃ HITP ₂	2	-	-	2-probe	-	10
[Cu ₃ (C ₆ S ₆)] _n	1,580	-	-	4-probe	0.00206	11
Cu ₃ BHS	110	-	-	4-probe	-	12
Cu ₃ HHTP ₂	1.5	-	-	4-probe	-	13
Cu-CAT-1	0.18	-	-	4-point	-	14
Ni ₃ TTB ₂	0.1	-	-	van der Pauw	0.041	15
[H ₂ N(CH ₃) ₂][Mn(HCO ₂) ₃]	4.237x10 ⁻¹	5.279 x10 ⁻¹	-	2-probe	0.00731	This work
[H ₂ N(CH ₃) ₂][Co(HCO ₂) ₃]	3.015 x10 ⁻¹	1.052 x10 ⁻¹	-	2-probe	0.01305	
[H ₂ N(CH ₃) ₂][Ni(HCO ₂) ₃]	4.872 x10 ⁻³	4.975 x10 ⁻¹	-	2-probe	0.01590	
[H ₂ N(CH ₃) ₂][Zn(HCO ₂) ₃]	4.785 x10 ⁻³	1.492 x10 ⁻¹	-	2-probe	0.01599	

H₂pdt = pyrazine- 2,3-dithiol, Hebic = 2-ethyl-1H-benzo[d]imidazole-5-carboxylic acid, H₂bdc = benzene-1,4-dicarboxylic acid, bpz = 3,3,5,5-tetramethyl-4,4-bipyrrozole, Hina = isonicotinic acid, DOBDC= 2,5-dioxybenzene-1,4-dicarboxylate, DSBDC= 2,5-disulfidobenzene-1,4-dicarboxylate, HIB= Hexaiminobenzene, HTB= Hexathiolbenzene, HITP=2,3,6,7,10,11-Hexaiminotriphenylene, BHS= Benzenehexaselenolate, HHTP= 2,3,6,7,10,11-hexahydroxytriphenylene, CAT= Catecholate, TTB= triamino-trithiolbenzene, E_a= activation energy.

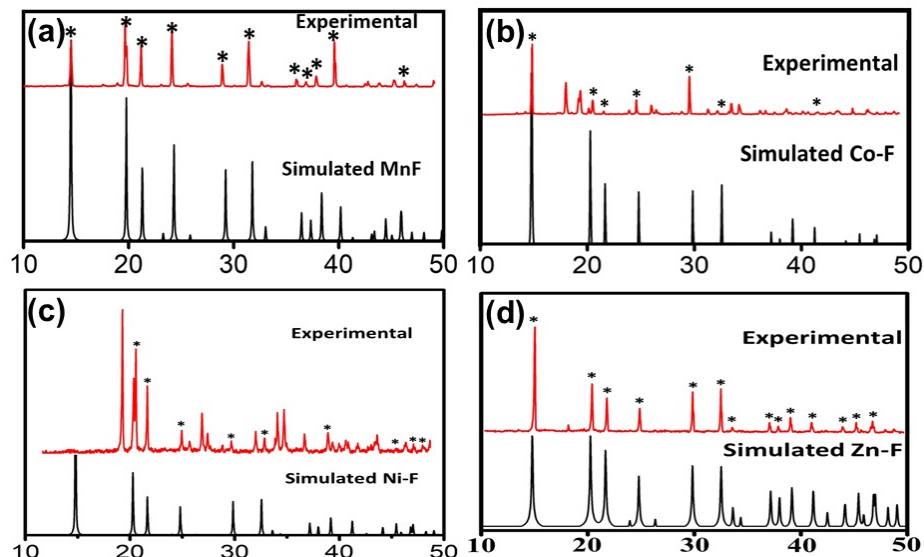


Fig S1: PXRD of (a) Mn-F, (b) Co-F, (c) Ni-F and (d) Zn-F MOFs; simulated (black) and experimental (red).

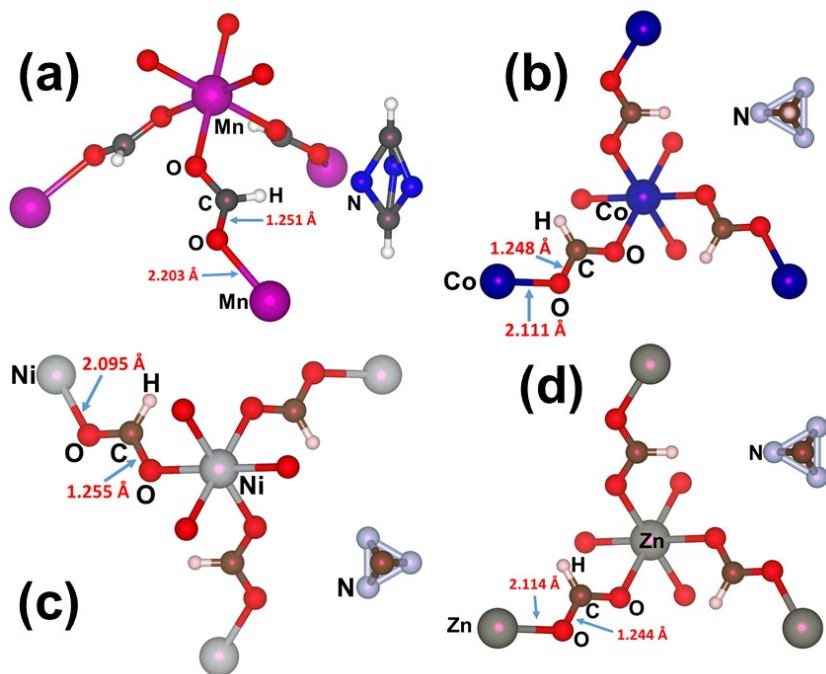


Fig S2: M-O and C-O bond lengths of (a) **Mn-F**, (b) **Co-F**, (c) Ni-F and (d) **Zn-F**.

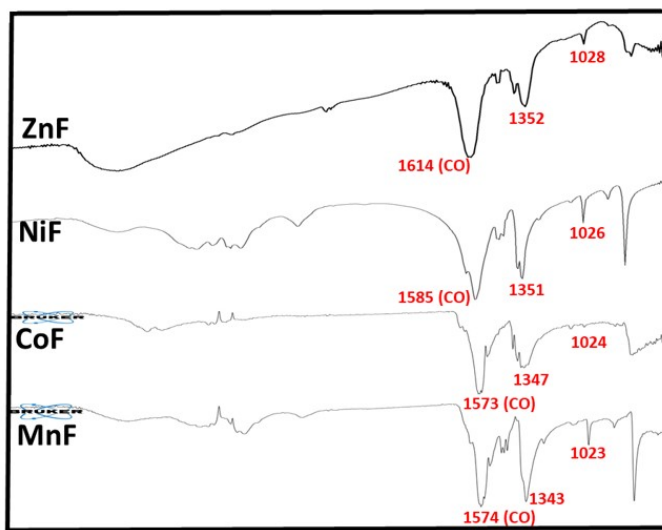


Fig S3: FTIR spectra of **Mn-F**, **Co-F**, **Ni-F** and **Zn-F** MOFs.

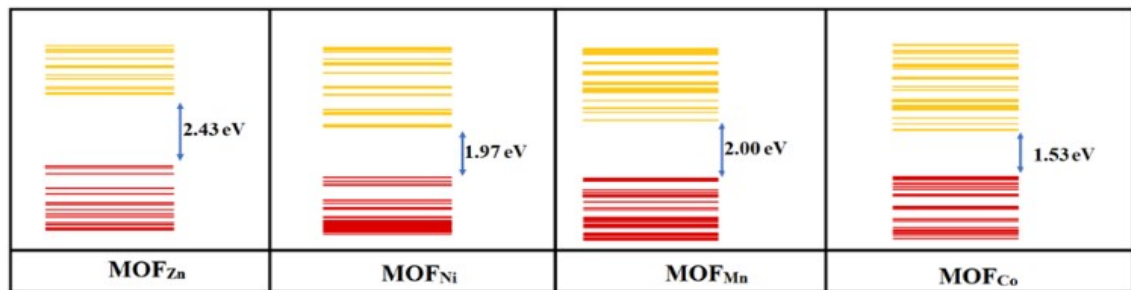


Fig S4: Calculated band gap (eV) of the MOFs.

Table S2: CO stretching frequency values of MOFs after and before heating.

MOF	Before heating, ν_{CO} in cm^{-1}	After heating, ν_{CO} in cm^{-1}
Mn-F	1574	1587
Co-F	1573	1585
Ni-F	1585	1587
Zn-F	1614	1630

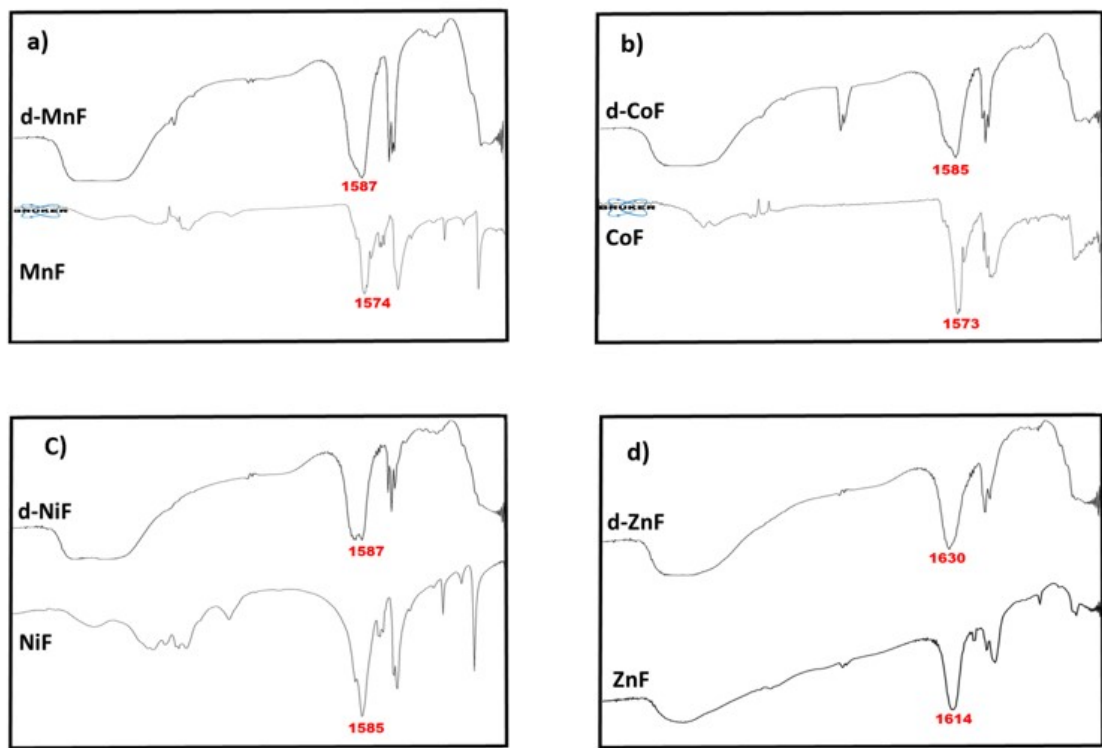
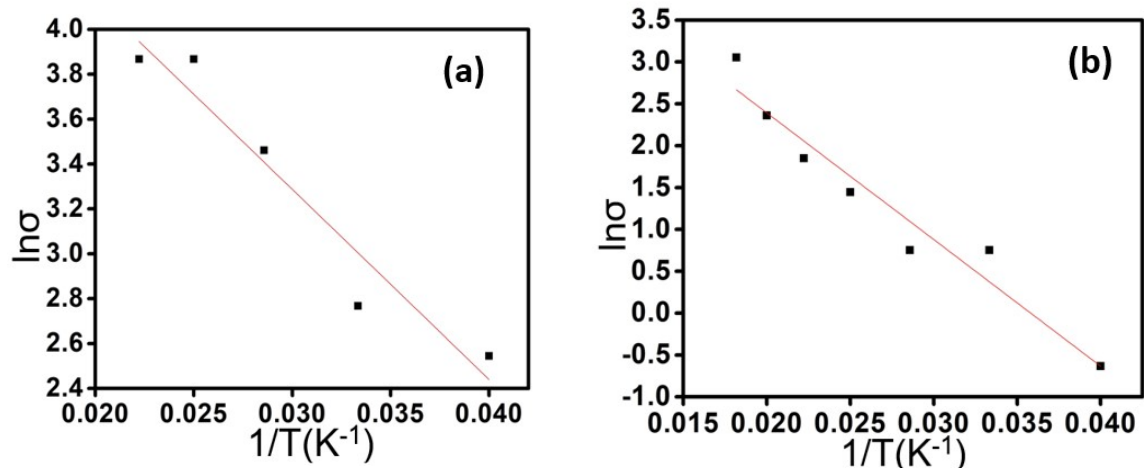
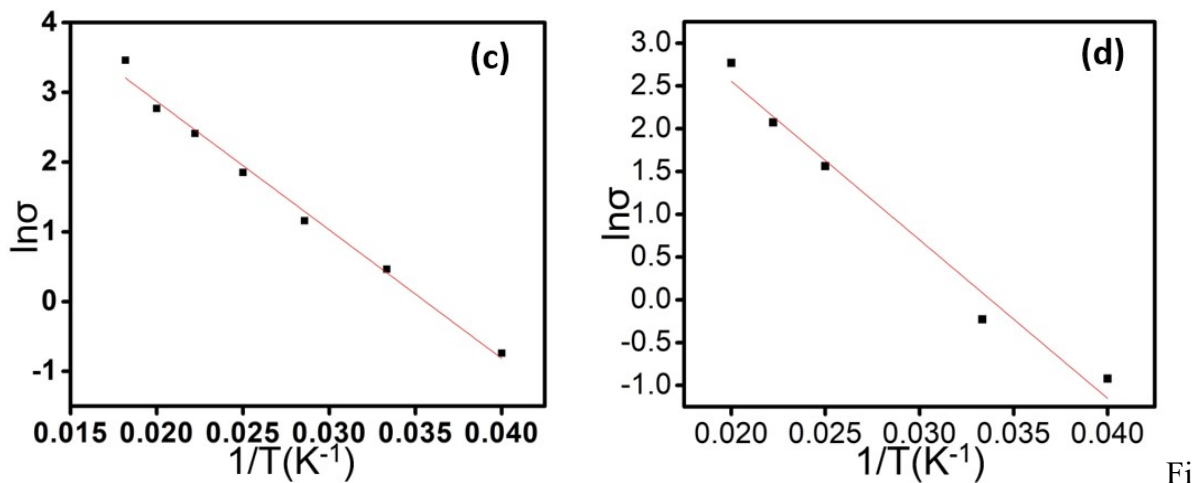


Figure S5: FTIR spectra C-O stretching frequencies before and after heating in (a) **Mn-F**, (b) **Co-F**, (c) **Ni-F** and (d) **Zn-F**.





S6: Temperature dependent conductivity curve of (a) **Mn-F**, (b) **Co-F**, (c) **Ni-F** and (d) **Zn-F** MOFs.

Fig

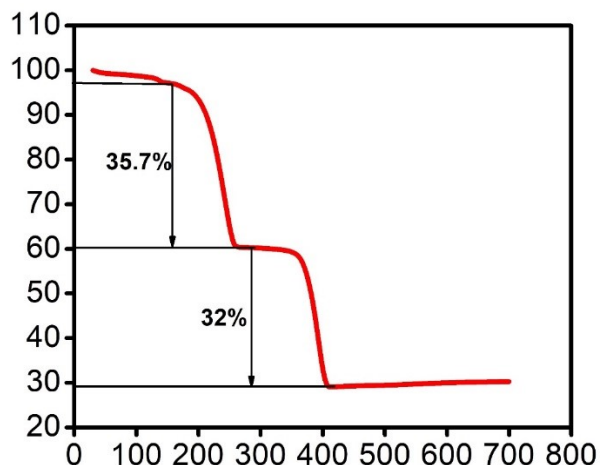


Fig S7: TGA graph of **Mn-F**.

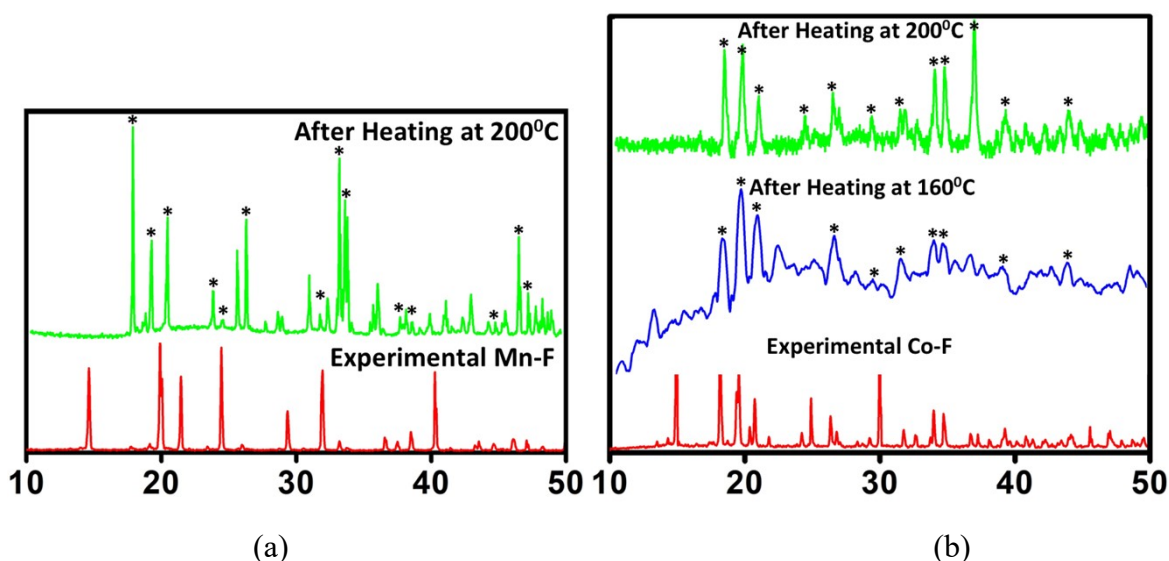


Fig S8: PXRD of (a) **Mn-F** and (b) **Co-F** before and after heating.

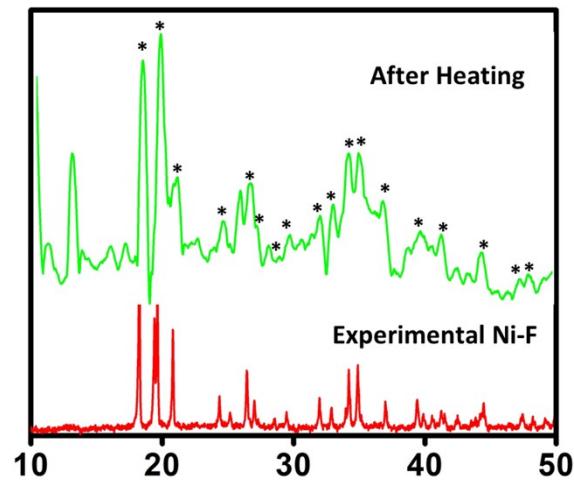


Fig S9: PXRD of Ni-F; simulated (black) and after heat (green) at 160 °C for 24 h.

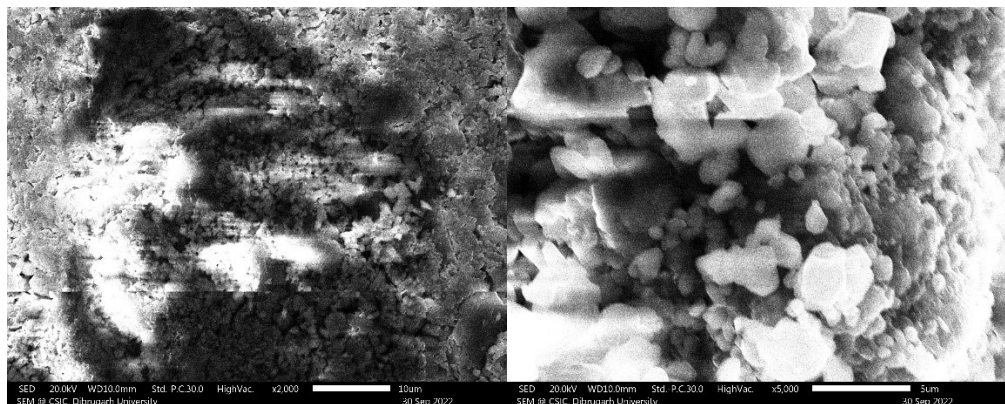


Figure S10: SEM image (2000X and 5000X) of the Co-F pellet.

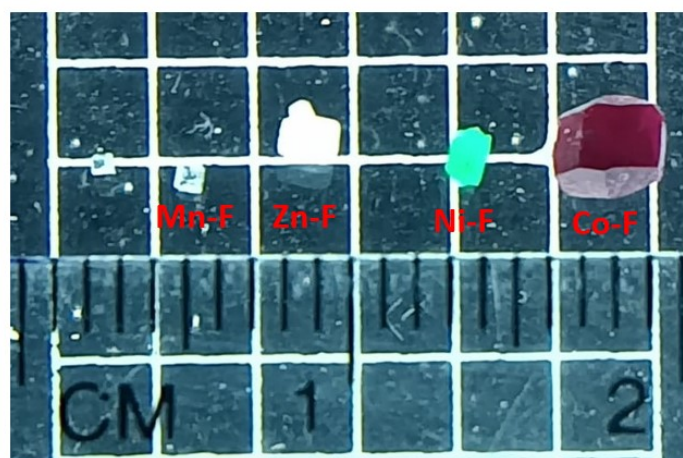


Fig S11: Single crystal images of the MOFs.

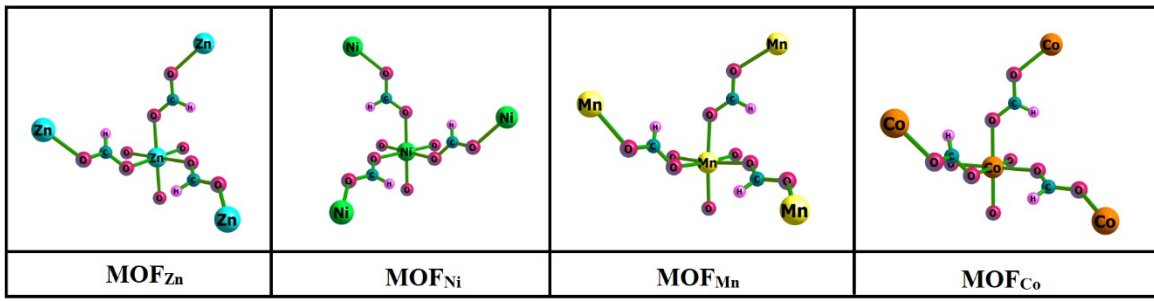


Fig S12: Optimized geometries of the Zn, Ni, Mn and Co containing Metal-Organic Frameworks.

Table S3: Crystallographic table

Compound No.	Mn-F	Co-F	Zn-F
Formulae	C ₁₅ H ₁₅ Mn ₃ N ₉ O ₁₈	C ₁₅ H ₉ Co ₃ N ₉ O ₁₈	C ₁₅ H ₉ N ₉ O ₁₈ Zn ₃
Mol. wt.	774.18	774.10	799.48
CCDC No	2263898	2263917	2263916
Crystal system	Trigonal	Trigonal	Trigonal
Space group	<i>R</i> -3 <i>c</i>	<i>R</i> -3 <i>c</i>	<i>R</i> -3 <i>c</i>
Temperature (K)	298 (2)	293(2)	293(2)
Wavelength (Å)	0.71073	0.71073	0.71073
<i>a</i> (Å)	8.3840(16)	8.1984(6)	8.1966(4)
<i>b</i> (Å)	8.3840(16)	8.1984(6)	8.1966(4)
<i>c</i> (Å)	23.021(6)	22.2560(17)	22.280(2)
α (°)	90.00	90.00	90.00
β (°)	90.00	90.00	90.00
γ (°)	120.00	120.00	120.00
V (Å ³)	1295.50(17)	1295.50(17)	1296.32(15)
Z	2	2	2
Density/gcm ⁻³	1.897	1.984	2.048
Abs. Coeff. /mm ⁻¹	1.428	1.447	2.884
Abs. correction	none	none	none
F(000)	768	672	792

Total no. of reflections	279	268	267
Reflections, $I > 2\sigma(I)$	277	267	263
Max. 2θ ($^{\circ}$)	25.24	25.21	25.13
Ranges (h, k, l)	-10 \leq h \leq 10 -10 \leq k \leq 10 -27 \leq l \leq 27	-9 \leq h \leq 9 -9 \leq k \leq 9 -26 \leq l \leq 26	-9 \leq h \leq 9 -9 \leq k \leq 9 -25 \leq l \leq 26
Completeness to 2θ (%)	0.976	1.000	1.000
Data/ Restraints / Parameters	279/0/ 28	268/0/ 25	267/0/ 25
Goof (F^2)	1.262	1.168	1.065
R indices [$I > 2\sigma(I)$]	0.0729	0.0553	0.0750
R indices (all data)	0.0730	0.0552	0.0755

References

- 1 L. Sun, C. H. Hendon, S. S. Park, Y. Tulchinsky, R. Wan, F. Wang, A. Walsh and M. Dinca, *Chem. Sci.*, 2017, **8**, 4450-4457.
- 2 L. Sun, C. H. Hendon, M. A. Minier, A. Walsh and M. Dinca, *J. Am. Chem. Soc.*, 2015, **137**, 6164-6167.
- 3 L. Sun, T. Miyakai, S. Seki and M. Dinca, *J. Am. Chem. Soc.*, 2013, **135**, 8185.
- 4 Y. Kobayashi, B. Jacobs, M. D. Allendorf and J. R. Long, *Chem. Mater.*, 2010, **22**, 4120-4122.
- 5 F. Yu, D. D. Li, L. Cheng, Z. Yin, M. H. Zeng and M. Kurmoo, *Inorg. Chem.*, 2015, **54**, 1655-1660.
- 6 G. P. Li, K. Zhang, H.Y. Zhao, L. Hou and Y. Y. Wang, *ChemPlusChem*, 2017, **82**, 716-720.
- 7 Y. Q. Hu, M. Q. Li, Y. Wang, T. Zhang, P. Q. Liao, Z. Zheng, X. M. Chen and Y. Z. Zheng, *Chem. Eur., J.* 2017, **23**, 8409-8413.

- 8 J. H. Dou, L. Sun, Y. Ge, W. Li, C. H. Hendon, J. Li, S. Gul, J. Yano, E. A. Stach and M. Dinca, *J. Am. Chem. Soc.*, 2017, **139**, 13608-13611.
- 9 T. Kambe, R. Sakamoto, K. Hoshiko, K. Takada, M. Miyachi, J. H. Ryu, S. Sasaki, J. Kim, K. Nakazato and M. Takata, *J. Am. Chem. Soc.*, 2013, **135**, 2462-2465.
- 10 D. Sheberla, L. Sun, M. A. Blood-Forsythe, S. Er, C. R. Wade, C. K. Brozek, A. Aspuru-Guzik and M. Dinca, *J. Am. Chem. Soc.*, 2014, **136**, 8859-8862.
- 11 X. Huang, P. Sheng, Z. Tu, F. Zhang, J. Wang, H. Geng, Y. Zou, C. Di, Y. Yi, Y. Sun, W. Xu and D. Zhu, *Nat. Commun.*, 2015, **6**, 7408.
- 12 Y. Cui, J. Yan, Z. Chen, J. Zhang, Y. Zou, Y. Sun, W. Xu and D. Zhu, *Adv. Sci.*, 2019, **6**, 1802235.
- 13 R.W. Day, D.K. Bediako, M. Rezaee, L.R. Parent, G. Skorupskii, M. Q. Arguilla, C. H. Hendon, I. Stassen, N. C. Gianneschi, P. Kim and M. Dincă, *ACS Cent. Sci.*, 2019, **5**, 1959-1964.
- 14 M. Hmadeh, Z. Lu, Z. Liu, F. Gándezara, H. Furukawa, S. Wan, V. Augustyn, R. Chang, L. Liao and F. Zhou, *Chem. Mater.*, 2012, **24**, 3511– 3513.
- 15 X. Sun, K. H. Wu, R. Sakamoto, T. Kusamoto, H. Maeda, X. Ni, W. Jiang, F. Liu, S. Sasaki, H. Masunaga and H. Nishihara, *Chem. Sci.*, 2017, **8**, 8078–8085.